PHYSICAL REVIEW E **70**, 050401(R) (2004)

Structural arrest transitions in fluids described by two Yukawa potentials

Jianlan Wu,[1] Yun Liu,[2] Wei-Ren Chen,[2] Jianshu Cao,[1] and Sow-Hsin Chen[2,*]
[1]*Department of Chemistry, Massachusetts Institute of Technology, Cambridge, Massachusetts 02139, USA*
[2]*Department of Nuclear Engineering, Massachusetts Institute of Technology, Cambridge, Massachusetts 02139, USA*
(Received 28 April 2004; published 15 November 2004)

We study a model colloidal system where particles interact via short-range attractive and long-range repulsive Yukawa potentials. Using the structure factor calculated from the mean-spherical approximation as the input, the kinetic phase diagrams as functions of the attraction depth and the volume fraction are obtained by calculating the Debye-Waller factors in the framework of the mode-coupling theory for three different heights of the repulsive barrier. The glass-glass reentrance phenomenon in the attractive colloidal case is also observed in the presence of the long-range repulsive barrier, which results in the lower and upper glass regimes. Competition between the short-range attraction and the long-range repulsion gives rise to new regimes associated with clusters such as "static cluster glass" and "dynamic cluster glass," which appear in the lower glass regime. Along the liquid-glass transition line between the liquid regime and the lower glass regime, crossover points separating different glass states are identified.

DOI: 10.1103/PhysRevE.70.050401 PACS number(s): 82.70.Dd, 83.80.Hj, 64.70.Pf

Recently, experiments and computer simulations on colloidal systems identify a local peak in the structure factor at a wave vector much smaller than that of the first diffraction peak (particle peak) [1,2]. This observation triggered much interest in the complex liquid community and raised fundamental questions regarding the nature of gelation, aggregation, and the glass transition [2–8]. Sciortino and co-workers found that the presence of long-range repulsive and short-range attractive potentials [2] leads to the aggregation of colloidal particles and results in a liquid-glass transition at low densities. Experiments on proteins and Laponite systems with these kinds of interactions revealed signatures of new cluster regimes [1,6,7]. In this Communication, we systematically study a model system with a short-range attractive and a long-range repulsive Yukawa potentials in addition to the hard-core potential. The structure factors are calculated by the mean-spherical approximation (MSA) [9,10], and the kinetic phase diagrams for the idealized liquid-glass transition are obtained in the framework of mode coupling theory (MCT) [11–13]. Liquids and glasses composed of clusters are analyzed in detail. Although the standard MCT is a first-order dynamic mean-field approximation [14,15], its predictions have been extensively verified in colloidal systems. For example, MCT predicts a liquid-glass transition at a critical volume fraction, $\phi^c \approx 0.516$, in the hard-sphere colloidal system [12], whereas the experimental result is around 0.58 [16]. The volume fraction is related to the number density ρ and the colloidal diameter σ by $\phi = \pi\rho\sigma^3/6$. A recent high-order MCT calculation by Wu and Cao [15] improves the prediction to $\phi^c = 0.552$. In attractive colloidal systems, MCT predicts repulsive and attractive glass states [17,18], which has been confirmed in experiments [19]. MCT is expected to provide reliable predictions, at least in the lowest order, in our model system.

Small angle x-ray scattering (SAXS) experiments on lysozyme solutions reveal that the protein-protein potential has a short-range attraction, and a long-range electrostatic repulsion [20] that can be described by a Yukawa form according to the DLVO [21] and GOCM [22] theories. With the unclear origin, the attraction has been simulated by different functional forms [2,20]. To exploit the known analytical form of S_q, we use a Yukawa form for the attraction part in our system, resulting in

$$\beta V(r) = \begin{cases} \infty, & 0 < r < 1 \\ -\dfrac{K_1 e^{-Z_1(r-1)}}{r} + \dfrac{K_2 e^{-Z_2(r-1)}}{r}, & r > 1, \end{cases} \quad (1)$$

where r is the dimensionless interparticle distance in units of σ, K_1 and Z_1 refer to the attraction, and K_2 and Z_2 refer to the repulsion. As in the screened Columbic potential, the inverse of the dimensionless repulsion range is given by the DLVO theory as $Z_2 = \kappa\sigma$ [21], where κ is the inverse of the Debye-Hückel screening length. The dependence of K_2 on both the ionic strength I and the particle charge z can be calculated by either DLVO [21] or GOCM [22].

The structure factor can be obtained by solving the Ornstein-Zernike equation with various closures. MSA is used in our calculations because the analytical solutions for Yukawa potentials were derived by Waisman and Stell [23], and Blum [9]. Following Blum's approach [9], we calculate the structure factor, which will be discussed in detail in a forthcoming paper [10]. Compared to other methods [24], our approach generates S_q efficiently over a broad range of wave vectors, which serves as a reliable input for our MCT calculations.

Before presenting kinetic phase diagrams, we discuss the dependence of S_q on the attraction depth K_1 and the repulsion range Z_2^{-1}. The structure factors are plotted for increasing K_1 in Fig. 1(a) for a set of parameters given as $Z_1 = 10$, $K_2 = 0.3$, $Z_2 = 0.5$, and $\phi = 0.3$. As the attraction strength grows, a cluster peak appears at a wave vector much smaller than that of the first diffraction peak (particle peak). As K_1 continues to increase to $K_1 = 10$, the strong attraction facilitates the aggregation process to form close-packing clusters. In Fig.

*Author to whom correspondence should be addressed. Email address: sowhsin@mit.edu

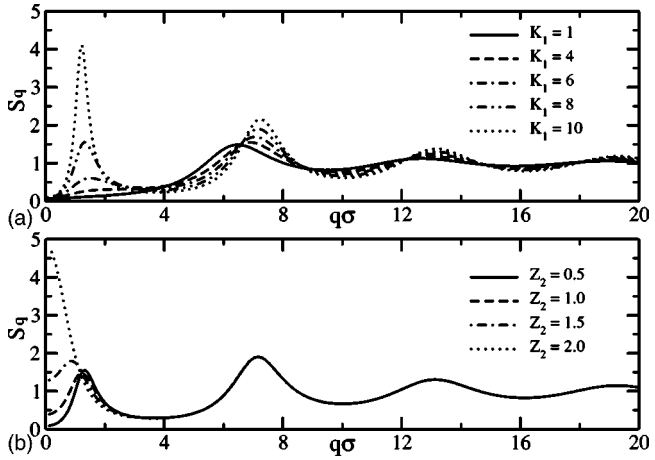

FIG. 1. (a) The structure factors for different attractive depths K_1 (see text). (b) The structure factors for different repulsive ranges Z_2^{-1} (see text).

1(b), the dependence of S_q on the repulsion range Z_2^{-1} is studied for fixed values of $K_1=8$, $Z_1=10$, $K_2=0.3$, and $\phi=0.3$. With the increase of Z_2 (the decrease of the repulsion range), the structure factor for $q \geqslant 4\sigma^{-1}$, including the particle peak, remains almost the same, but the cluster peak quickly shifts to a lower wave vector with the increasing intensity and eventually diverges at $q=0$. This result demonstrates that clusters grow with decreasing range of repulsion. With a strong attraction depth, we expect to observe a gel phase, where colloidal particles form a percolating network.

In the remainder of this Communication, we will fix Z_1 and Z_2 and study the kinetic phase diagram as a function of K_1 and ϕ for three values of K_2. Three repulsive heights are employed: $K_2=0.3$, 1, and 5, where the corresponding particle charges in the DLVO theory are $z=1.5$, 2.7, and 6, respectively. We set $Z_2=0.5$, which corresponds to a weak ionic strength of $I=2.1$ mM and $\sigma=33$ Å, and $Z_1=10$, because the attraction range in the protein systems is around 10% of the hard-sphere diameter [20]. Following the discussion on Fig. 1, we expect that the sizes of clusters are finite. The dependence on Z_1 and Z_2 will be addressed in a future work.

Using the analytical structure factor S_q as the input, we employ the standard MCT [11–13] to calculate the Debye-Waller (nonergodic) factor f_q, defined as the normalized long time limit of the coherent intermediate scattering function, $f_q=\lim_{t\to\infty}F_q(t)/S_q$. The corresponding high-order MCT calculations [15] will be investigated in the future. A central result of MCT is the self-consistent equation for f_q, which predicts the idealized liquid-glass transition [12]. When a system is in the liquid state (ergodic), only the trivial solution, $f_q=0$, exists, but when the system is in the glass state (nonergodic), another nontrivial solution, $f_q>0$, appears. The transition point in the parameter space is determined by the discontinuity of f_q from zero to a nonvanishing value. To obtain f_q in our system, we follow the numerical method in Ref. [13].

The kinetic phase diagrams are plotted for three K_2 in Figs. 2(a)–2(c), where the horizontal axis is the volume fraction ϕ and the vertical axis is the inverse of the attraction depth, K_1^{-1}. Similar to attractive colloidal systems [18], the liquid regime (LR) is surrounded by the upper glass regime (UGR) and lower glass regime (LGR). As shown in Figs. 2(b) and 2(c), increasing the repulsion strength extends the liquid phase to larger ϕ and K_1 because the system requires stronger attraction to trap colloids or higher volume fraction to form arrested cages. The glass-glass reentrance phenomenon occurs at $\phi \geqslant 0.516$, where the transition line between the LR and UGR appears. When the attraction is weak, the cage effect induced by high ϕ dominates and the system is in the UGR, similar to the repulsive glass in the attractive colloidal suspensions [18]. Because the colloidal particles move closer as attraction increases, the collective motions recover the ergodicity and the system enters the liquid phase. When

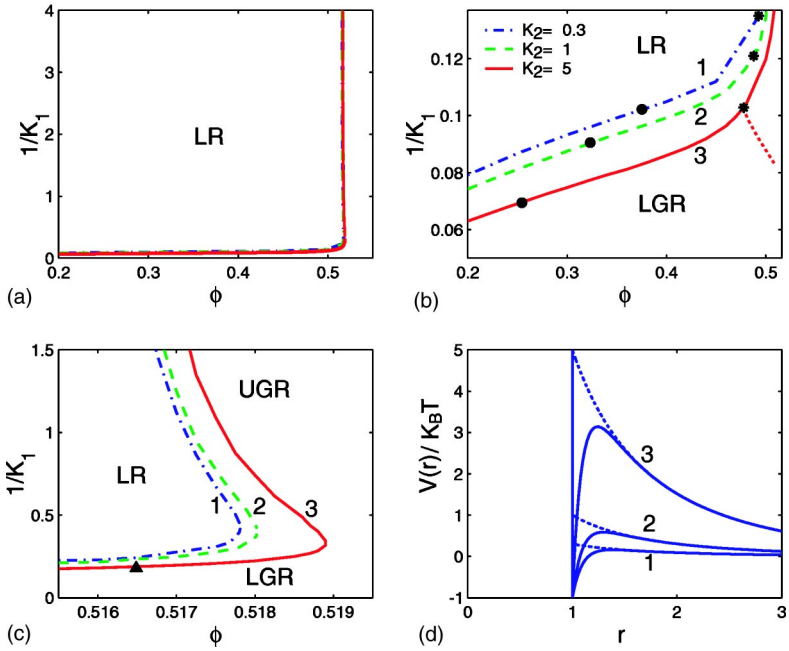

FIG. 2. Kinetic phase diagrams and potentials for $Z_1=10$ and $Z_2=0.5$. Curves labeled by 1, 2, and 3 correspond to $K_2=0.3$, 1, and 5, respectively. (a) Kinetic phase diagrams are shown in a wide range of ϕ and K_1^{-1}. (b) The lower part of (a) to show the transition between the LR and LGR. The stars mark the crossover from the static cluster glass to the dynamic cluster glass (see text). The dotted line demonstrates the separation of these two cluster glass states inside LGR for $K_2=5$. The solid circles mark ϕ where the cluster peaks are equal to the particle peaks in S_q. (c) Another part of (a) close to the ending point of LR to mark the termination of the dynamic cluster glass. (d) Potential surfaces for different K_1 and K_2. Line 1 is for $K_2=0.3$ and $K_1=1.3$. Line 2 is for $K_2=1$ and $K_1=2$. Line 3 is for $K_2=5$ and $K_1=6$. The dotted lines correspond to the pure long-range repulsion.

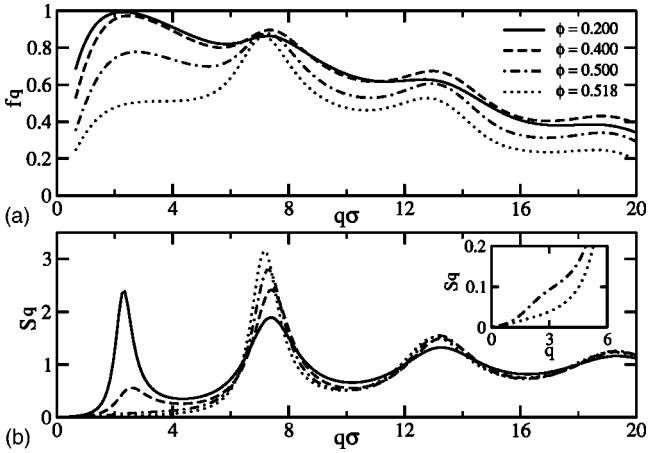

FIG. 3. (a) Four Debye-Waller factors f_q along the transition line between the liquid regime (LR) and the lower glass regime (LGR) for $K_2=5$. (b) The structure factor S_q corresponding to the same parameters in (a).

the attraction is sufficiently strong, colloid particles are randomly trapped by potential wells deeper than thermal fluctuations, and the system enters the LGR. Although sharing a similar mechanism, the LGR for the two Yukawa potential is more complicated than the attractive glass state in the attractive colloidal system [18]. For the parameters chosen in this paper, we test $K_1>30$, and $S_{q=0}$ does not diverge, indicating that the spinodal line is far below the transition line between the LR and LGR. The binodal lines are more complicated and will be investigated in future work.

Clusters in the liquid and glass states of our systems are stabilized by the competition between the short-range attraction and long-range repulsion [2,5,6,8]. Based on microscopic descriptions with S_q and f_q, we now discuss these cluster states in detail. In Fig. 3, the structure factors and the corresponding Debye-Waller factors along the transition line between the LR and LGR are plotted for $K_2=5$ and for four values of ϕ ranging from 0.2 to 0.518. In addition to the particle peak at $q_m \approx 7.3\sigma^{-1}$, we observe the cluster peak in several S_q and f_q curves at a much smaller wave vector, $2.3\sigma^{-1}<q'_m<3.3\sigma^{-1}$. We discuss separately four states in Fig. 3. (i) For $\phi=0.2$, the cluster peaks are higher than the particle peaks in both S_q and f_q, and $f_{q'_m}$ is equal or close to one, indicating that colloidal particles aggregate into stable close-packing clusters. The characteristic size of clusters is finite due to the balance of the attraction and repulsion. Because of their thermal and dynamic stability, close-packing clusters are the basic units of the system instead of colloidal monomers. As a result, it is possible to improve our predictions for low volume fractions using the effective cluster description proposed recently [8]. Characterized by the presence of the cluster peak in S_q, the ergodic state can be viewed as a cluster liquid, the nonergodic state discussed here is a "**static cluster glass.**" (ii) For $\phi=0.4$, we observe $S_{q'_m} \ll S_{q_m}$ and $1 \approx f_{q'_m} > f_{q_m}$. Compared to the case of $\phi=0.2$, the cluster population substantially decreases, suggesting that the cluster structures are less ordered. The large cluster peak in f_q indicates that the less-ordered cluster structure remains dynamically more stable than single colloids. Because the calculation is carried out along the transition line between the LR and LGR in Fig. 2(b), the attraction strength K_1 decreases as ϕ increases. The disordered cluster structure is related to the decrease of the strength and effective width of the attractive well. Compared to experiments and schematic phase diagrams [3,6], the glass states at $\phi=0.4$ and 0.2 may be the precursors of the gel state in Ref. [6], which is an infinite percolating network resulting from the growth of the finite-size clusters in our system. (iii) For $\phi=0.5$, we observe an inflection point instead of a cluster peak at $q \approx 3.2\sigma^{-1}$ in S_q, as shown in the inset of Fig. 3(b), and the cluster peak in f_q is smaller than the particle peak. Affected by both the increase in ϕ and the decrease in K_1, the cluster structure is highly disordered and does not have a characteristic size. However, the cluster peak in f_q suggests that disordered cluster structures in the glass state are dynamically selected with a characteristic cluster size. The wave vector of the cluster peak in f_q is smaller than the inflection point in S_q, indicating that clusters are more likely to result from dynamics than thermodynamics. These cluster structures may be related to the heterogeneous structures in the activation picture of glass formation [25,26]. Following these arguments, we consider this glass state as a "**dynamic cluster glass.**" (iv) For $\phi=0.518$, the cluster peaks in both S_q and f_q disappear. With the attraction depth of $K_1=4.5$, we have $\beta V(r=1^+)>0$ so the binary bond between two colloidal particles is unstable and will dissociate. As a result, the probability of forming stable clusters is small and the basic dynamic unit in the glass state is a single colloidal particle.

We now extend the above discussion of Fig. 3 for one value of K_2 to several values of the repulsion strength. Figure 4 is a plot of the cluster and particle peaks in S_q and f_q along the transition line between the LR and LGR for $K_2=0.3$, 1, and 5, respectively. The basic behaviors of the peak values are similar for different K_2. With the rapid decrease of $S_{q'_m}$, the cluster peak in f_q remains close to one for $\phi \leqslant 0.4$, but quickly decreases around $0.45<\phi<0.5$. Interestingly, as $f_{q'_m}$ becomes smaller than f_{q_m}, the cluster peak in S_q turns into an inflection point, indicating a crossover from the static to the dynamic cluster glass regimes. We define the crossover density ϕ_1 between the two regimes by the disappearance of the cluster peak in S_q, giving $\phi_1(K_2=0.3)=0.49$, $\phi_1(K_2=1)=0.48$, and $\phi_1(K_2=5)=0.47$, denoted by stars in Fig. 2(b). These values of ϕ_1 are close to the freezing point, 0.49, of hard-sphere fluids [16]. This coincidence implies a possible connection between cluster aggregation and crystallization. To demonstrate the tendency for the separation of these two cluster glass states inside LGR, a calculation for $K_2=5$ is provided as the dotted line in Fig. 2(b). The termination of the dynamic cluster glass regime is marked by the disappearance of the cluster peak in f_q, which defines another crossover density ϕ_2. For the weak repulsive strength, e.g., $K_2=0.3$ and 1, the attractive well remains negative in the glass regime, excluding the observation of ϕ_2. For the strong repulsive potential $K_2=5$, the crossover density is $\phi_2(K_2=5)=0.5165$, denoted by a triangle in Fig. 2(c). Although the above conclusions drawn from f_q and S_q are crude, future studies will also investigate other measures to explore cluster formation in different regimes.

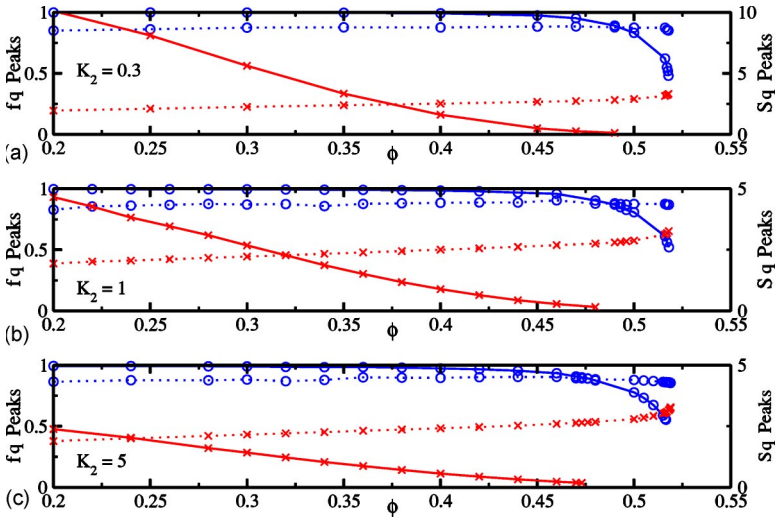

FIG. 4. This figure summarizes the intensity changes of the cluster peaks and the particle peaks in f_q and S_q along the transition line between the LR and LGR. Lines with circles denote peaks in f_q, referring to the left vertical axes, and lines with crosses denote peaks in S_q, referring to the right vertical axes. The solid lines are the cluster peaks, whereas the dotted lines are the particle peaks.

In summary, we study the structural arrest transitions in a model system with a short-range attractive and a long-range repulsive Yukawa potentials. Based on Blum's approach [9], an efficient method is developed to obtain the structure factor for the two-Yukawa system [10]. The calculated structure factor shows that the intensity of the cluster peak in S_q increases as the depth of the attraction increases and the cluster peak shifts to the zero wave vector as the range of the repulsion decreases. By computing the Debye-Waller factor f_q from the standard MCT [11–13], we obtain the kinetic liquid-glass phase diagrams and observe the glass-glass reentrance phenomenon. The detailed studies of cluster peaks and particle peaks in S_q and f_q along the transition line between the liquid regime and the lower glass regime reveal different cluster regimes in our system, most notably the static cluster glass and the dynamic cluster glass. Our results confirm and significantly extend recent computer simulation results of Sciortino *et al.* [2] and experiments by Tanaka *et al.* [6]. More studies are required to investigate detailed mechanisms for forming different cluster regimes as well as their relationships to the gel phase and attractive glass phase. As shown in Fig. 1, the ranges of attraction and repulsion strongly affect the characteristic size of clusters. Following this line of research, we hope to find the connection between the gelation process, which forms a network with an infinite size, and the aggregation process, which forms clusters with finite sizes.

S.H.C. acknowledges the support of a grant from the Materials Science Division of U.S. DOE, Contract No. DE-FG02-90ER45429. S.H.C. benefits from affiliation with the EU funded Marie-Curie Network on Arrested Matter. J.C. acknowledges the support of the NSF and the Camille Dreyfus Foundation.

[1] B. Lonetti, E. Fratini, S. H. Chen, and P. Baglioni, Phys. Chem. Chem. Phys. **6**, 1388 (2004).
[2] F. Sciortino *et al.*, e-print cond-mat/0312161.
[3] F. Sciortino, Nat. Mater. **1**, 145 (2002).
[4] K. A. Dawson, Curr. Opin. Colloid Interface Sci. **7**, 218 (2002).
[5] J. Groenewold and W. K. Kegel, J. Phys. Chem. B **105**, 11702 (2001).
[6] H. Tanaka *et al.*, Phys. Rev. E **69**, 031404 (2004); R. P. Sear *et al.*, *ibid.* **59**, R6255 (1999).
[7] B. Ruzicka, L. Zulian, and G. Ruocco, J. Phys.: Condens. Matter (to be published).
[8] M. E. Cates *et al.*, e-print cond-mat/0403684.
[9] J. S. Høye and L. Blum, J. Stat. Phys. **16**, 399 (1977).
[10] Y. Liu *et al.*, J. Chem. Phys. (to be published).
[11] E. Leutheusser, Phys. Rev. A **29**, 2765 (1984).
[12] W. Götze and L. Sjögren, Prog. Phys. **55**, 241 (1992).
[13] T. Franosch, M. Fuchs, W. Götze, M. R. Mayr, and A. P. Singh, Phys. Rev. E **55**, 7153 (1997).
[14] J. S. Cao, J. L. Wu, and S. L. Yang, J. Chem. Phys. **116**, 3739 (2002); J. L. Wu and J. S. Cao, Phys. Rev. E **67**, 061116 (2003).
[15] J. L. Wu and J. S. Cao (unpublished).
[16] P. N. Pusey and W. van Megen, Nature (London) **320**, 340 (1986).
[17] J. Bergenholtz and M. Fuchs, Phys. Rev. E **59**, 5706 (1999).
[18] K. Dawson *et al.*, Phys. Rev. E **63**, 011401 (2000).
[19] S. H. Chen *et al.*, Science **300**, 619 (2003).
[20] A. Tardieu, S. Finet, and F. Bonneté, J. Cryst. Growth **232**, 1 (2001); M. Malfois *et al.*, J. Chem. Phys. **105**, 3290 (1996).
[21] E. J. W. Verwey and J. TH. G. Overbeek, *Theory of the Stability of Lyophobic Colloids* (Elsevier, Amsterdam, 1948).
[22] C. Wu and S. H. Chen, J. Chem. Phys. **87**, 6199 (1987).
[23] J. S. Høye, G. Stell, and E. Waisman, Mol. Phys. **32**, 209 (1976); E. Waisman, J. S. Høye, and G. Stell, Chem. Phys. Lett. **40**, 514 (1976).
[24] J. Konior and C. Jedrzejek, Mol. Phys. **48**, 219 (1983).
[25] C. A. Angell, J. Phys.: Condens. Matter **12**, 6463 (2000).
[26] X. Xia and P. G. Wolynes, Proc. Natl. Acad. Sci. U.S.A. **97**, 2990 (2000); Phys. Rev. Lett. **86**, 5526 (2001).